Supporting Information

Fei et al. 10.1073/pnas.1412922111

SI Methods

Purification of GroEL^{WT}, GroEL^{E315C}, GroES^{WT}, and GroES^{98C}. These proteins were prepared, purified, and labeled as previously described (1). Typically, GroEL preparations contained <0.2 mol contaminating substrate protein per mole $GroEL_{14}$ (i.e., <10% of the rings may be contaminated with an ensemble of substrate proteins). The concentrations of purified GroEL and GroES were measured at 280 nm using the extinction coefficients of 9,600 $cm^{-1}{\cdot}M^{-1}$ and 1,200 $cm^{-1}{\cdot}M^{-1}$, respectively.

Preparation of Denatured Rubisco and Malate Dehydrogenase. Rubisco (ribulose-1,5-bisphosphate carboxylase oxygenase) was overexpressed from a plasmid containing His-tagged Rubisco from *Rhodospirillum rubrum*, a gift from Grant Pearce (Canterbury University, Christchurch, New Zealand), and purified in essentially the same way as GroES^{his} (1). Malate dehydrogenase (MDH) from pig heart mitochondria was purchased from Roche Applied Science. The concentrations of Rubisco and MDH were measured at 280 nm using the extinction coefficients of 67,000 $cm^{-1}{\cdot}M^{-1}$ and 6,800 $cm^{-1}{\cdot}M^{-1}$, respectively. Rubisco was denatured by incubating a 20–30 μM Rubisco solution with 8 M freshly made acid urea (20 mM glycine·HCl, pH 2.5) for 10 min on ice.

Labeling GroEL^{E315C}, GroES^{98C}, MDH, and Rubisco. A slight modification of the method described by Rye (2) was used to label GroEL^{E315C} with IAEDANS [5-((((2-iodoacetyl)amino)ethyl)amino) naphthalene- 1-sulfonic acid] and GroES98C with fluorescein-5-maleimide (F5M). MDH^{QSY7} was prepared as follows: 100 μM denatured MDH in freshly made urea was mixed with 110 μM QSY-7 maleimide (Sigma Aldrich) and incubated while agitating in the dark for 1 h at room temperature. Unreacted dye was removed by extensive washing using an YM-10 microcon (Millipore Corporation). The extent of labeling (~1 mol QSY7/mol MDH subunit) was measured at 560 nm to determine the dye concentration and Bradford assay for MDH concentration. The extinction coefficient used for the QSY-7 is 90,000 $cm^{-1}{\cdot}M^{-1}$. Rubisco was labeled as described in ref. 2 with minor modifications.

Preparation of Asymmetric "Resting State" and "Acceptor State" Complexes of GroEL–GroES$_1$. These complexes were prepared following the same method as described before (1, 3, 4).

Stopped-Flow Measurements of Substrate Protein Encapsulation. FRET-based measurements at 37 °C using GroES^{F5M} and the MDH/Rubisco^{QSY7} to track the encapsulation of substrate protein were conducted as described in corresponding figure legend, similar in principle to those previously described (1, 2). The calibration of the system is shown in Fig. 3*A*.

Crystallization. The MT-football complex GroEL:$GroES_2$ was made by mixing 150 μM GroEL^{wt}, 900 μM GroES^{wt}, 3.6 mM ATP, 4.8 mM $BeCl_2$, and 48 mM KF in Buffer A [50 mM Tris-acetate (pH 7.5), 20 mM $MgCl_2$, and 200 mM KCl]. Crystals containing both GroEL and GroES were first grown in 25% PEG 550 monomethyl ether (mme) (vol/vol) and 0.1 M Tris·HCl buffer, pH 8.5. In the crystal optimization that followed, diffraction-quality crystals were grown in 8.5% PEG 550 mme (vol/vol) and 0.1 M acetic acid-KCl buffer, pH 5.0. These crystals took about 10 d to fully grow and reach their maximum size, ~1 × 0.5 × 0.5 mm. Before crystals were mounted, they were removed from the mother liquor and soaked in dehydration buffer [12% PEG 550 mme (vol/vol), 20% ethylene glycol, 0.1 M acetic acid (pH 5.25), 20 mM $MgCl_2$, 200 mM KCl, 1 mM $BeCl_2$, and 10 mM KF] for 3–7 min.

The Rubisco-containing football complex GroEL–$GroES_2$–$Rubisco_2$ [substrate protein (SP) football] was made by first mixing 150 μM GroEL^{wt}, 900 μM GroES^{wt}, and 42 μM acid-denatured Rubisco-His6 in Buffer A. The protein mixture was held at room temperature for 15 min. After that, ATP (3.6 mM), $BeCl_2$ (4.8 mM), and KF (48 mM) were added into the protein mixture. Crystals of SP football were obtained under conditions similar to those of the MT football. Single cubic-shaped crystals were mounted after a similar dehydration procedure.

Data Collection and Structure Determination. Diffraction data of the SP-free football complex was collected at Northeastern Collaborative Access Team (NE-CAT) beamline 24-ID-E located at the Advanced Photon Source, Argonne National Laboratory. Three hundred frames with 0.5° oscillation were collected at 100 K. The data were indexed and integrated using iMOSFLM (5). The structure was solved by segmented molecular replacement. Seven search models were fitted one at a time. Each model consisted of one GroEL subunit and one GroES subunit extracted from the *cis* ring of GroEL-$GroES_1$-ADP_7 (1AON).

Diffraction data for the SP-football complex were collected at NE-CAT beamline 24-ID-C located at the Advanced Photon Source, Argonne National Laboratory. Nine hundred frames with 0.2° oscillation were collected at 100 K. The datasets were indexed and integrated using iMOSFLM (5). The structure was solved by molecular replacement using the MT-football complex as the search model.

Structural refinements of the MT-football and SP-67 football complexes were performed with the PHENIX suite (6). Refinement strategies include individual coordinates, rigid body, individual b factors, and translation/libration/screw, with torsion-angle noncrystallographic symmetry restraints, secondary structure restraints, and Ramachandran restraints. In the last two cycles of refinements the Ramachandran restraints were released. Over 96% of residues in the model of MT football and SP football are within the favored regions of the Ramachandran plot. The asymmetric unit of both MT and SP footballs contain a full functional unit: $GroEL_{14}$-$GroES_{14}$.

The conformational differences between MT football and SP football are very small and within experimental error (Fig. S5). To exclude the possibility that model bias causes such similarity, we redid the molecular replacement of the SP football using a slightly disturbed model of the MT football. After five cycles of refinement using the strategies described before, the resulting model of SP football is nearly identical to the final model (rmsd = 0.35).

1. Grason JP, Gresham JS, Widjaja L, Wehri SC, Lorimer GH (2008) Setting the chaperonin timer: The effects of K^+ and substrate protein on ATP hydrolysis. *Proc Natl Acad Sci USA* 105(45):17334–17338.
2. Rye HS (2001) Application of fluorescence resonance energy transfer to the GroEL-GroES chaperonin reaction. *Methods* 24(3):278–288.
3. Ye X, Lorimer GH (2013) Substrate protein switches GroE chaperonins from asymmetric to symmetric cycling by catalyzing nucleotide exchange. *Proc Natl Acad Sci USA* 110(46):E4289–E4297.
4. Yang D, Ye X, Lorimer GH (2013) Symmetric GroEL:$GroES_2$ complexes are the protein-folding functional form of the chaperonin nanomachine. *Proc Natl Acad Sci USA* 110(46):E4298–E4305.
5. Battye TGG, Kontogiannis L, Johnson O, Powell HR, Leslie AGW (2011) iMOSFLM: A new graphical interface for diffraction-image processing with MOSFLM. *Acta Crystallogr D Biol Crystallogr* 67(Pt 4):271–281.
6. Adams PD, et al. (2010) PHENIX: A comprehensive Python-based system for macromolecular structure solution. *Acta Crystallogr D Biol Crystallogr* 66(Pt 2):213–221.

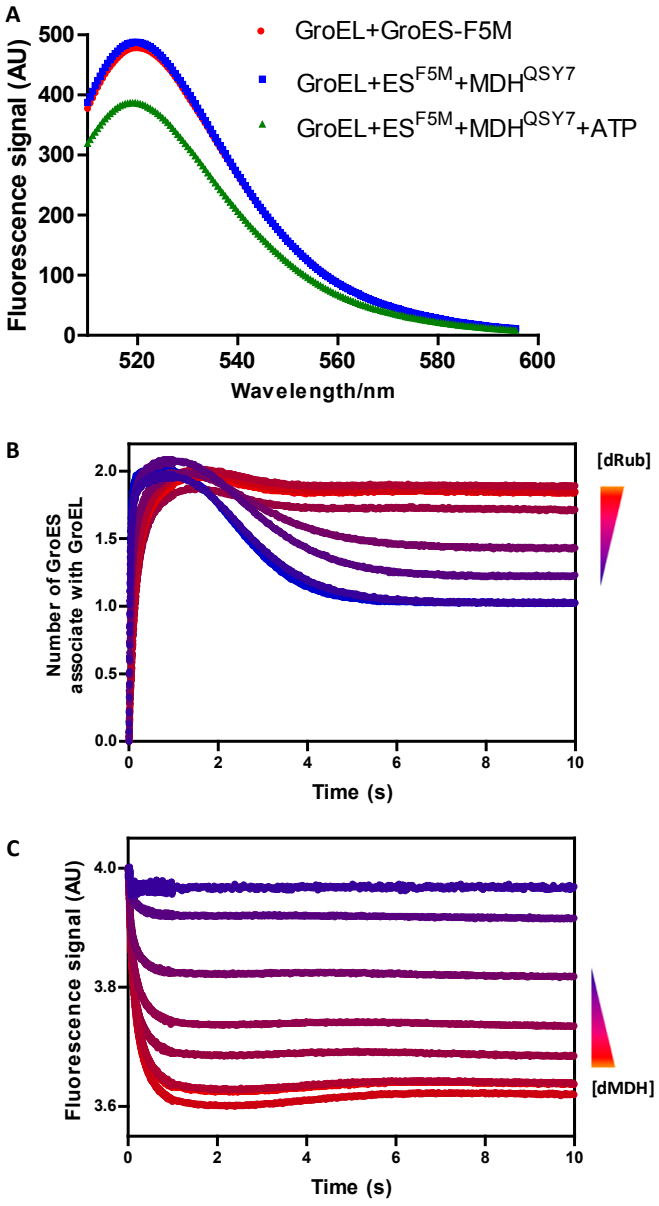

Fig. S1. (*A*) Steady-state fluorescence quenching of GroES^{F5M} by dMDH^{QSY7}. Quenching of GroES^{F5M} only occurs in the presence of d-MDH^{QSY7}, ATP and GroEL; 2 μM GroEL^{wt}, 3 μM GroES^{F5M}, 0.429 μM dMDH^{QSY7}, and 0.5 mM ATP were used. (*B*) Pre-steady-state formation of GroEL:GroES$_2$ monitored by FRET in the presence of denatured Rubisco. The experiments were performed in essentially the same way as those summarized in Fig. 2*A*, and the steady-state level of football were plotted against corresponding [dRubisco] shown in Fig. 2*C*. (*C*) Encapsulation of dRubisco by GroEL:GroES$_2$ shown by titrating GroEL ring with dRubisco^{QSY7} reported by the quenching of F5M-labeled GroES. The experiments were performed in essentially the same way as those summarized in Fig. 2*B*, and the summary plot was shown in Fig. 2*C*.

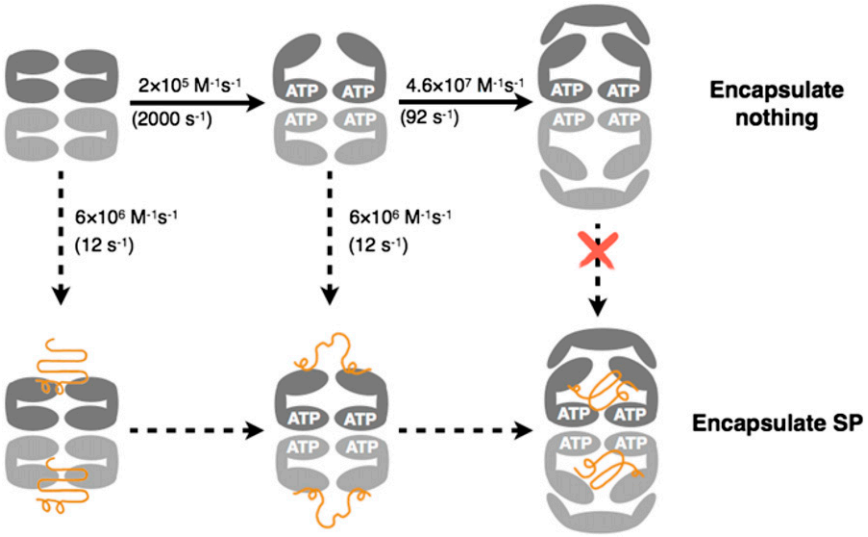

Fig. S2. An alternative mechanism of chaperonin–nucleotide exchange. This proposal (1) is based on the results of experiments performed in the absence of GroES and purports to describe the situation in vivo. The second-order rate constants are experimentally determined values; the pseudofirst-order constants in parentheses were obtained using values for the [ATP] and [SP] in vivo in *Escherichia coli* of 10 mM and 2 μM (set as equivalent to the in vivo $[GroEL]_7$), respectively (2, 3). However, this analysis is conceptually flawed for it fails to consider the subsequent binding of GroES and SP to the binary GroEL–ATP complex. Because the second-order rate constant for the binding of GroES to GroEL–ATP (4.6×10^7 $M^{-1} \cdot s^{-1}$) is almost 10-fold greater than that for the binding of SP, this mechanism leads to the formation of the biologically unproductive ternary complex GroEL–ATP–GroES, which precludes the binding of SP.

1. Tyagi NK, Fenton WA, Horwich AL (2009) GroEL/GroES cycling: ATP binds to an open ring before substrate protein favoring protein binding and production of the native state. *Proc Natl Acad Sci USA* 106(48):20264–20269.
2. Bennett BD, et al. (2009) Absolute metabolite concentrations and implied enzyme active site occupancy in Escherichia coli. *Nat Chem Biol* 5(8):593–599.
3. Lorimer GH (1996) A quantitative assessment of the role of the chaperonin proteins in protein folding in vivo. *FASEB J* 10(1):5–9.

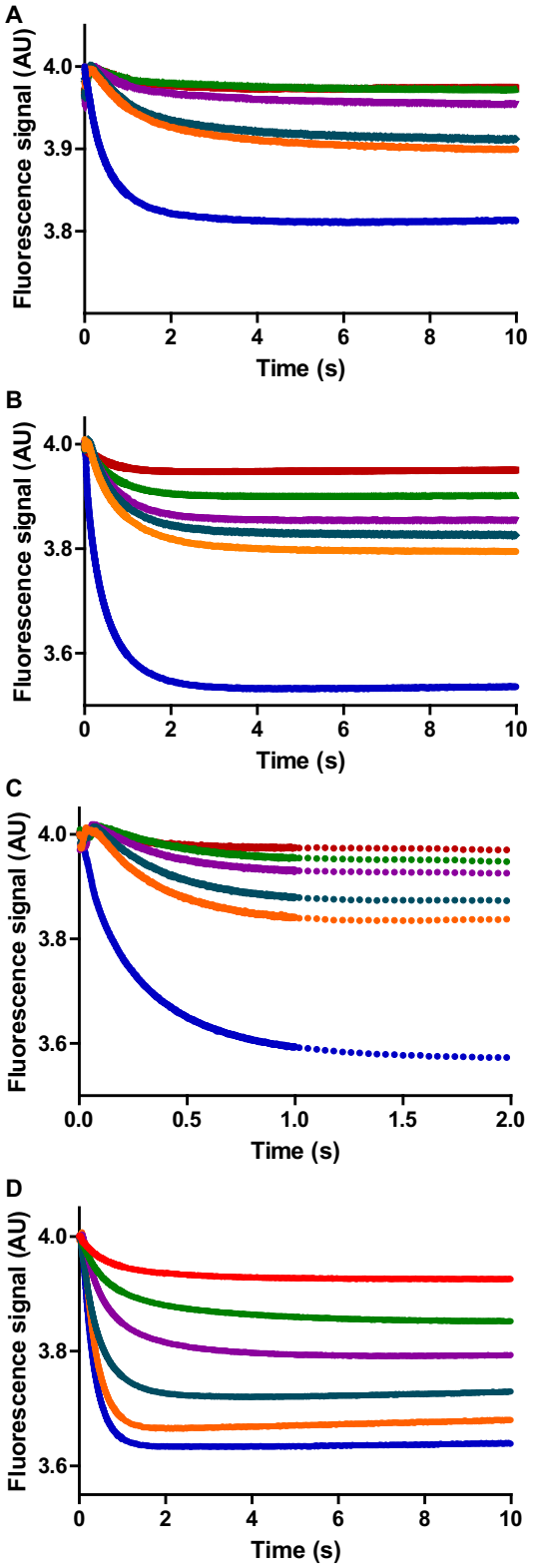

Fig. S3. The experimental consequences of permitting ATP to bind to GroEL before SP (QSY7-MDH) and F5M-GroES; 2 μM of (*A*) the *trans* ring of the acceptor state complex, (*B*) apo-GroELD398A, (*C*) apo-GroEL^{wt}, or (*D*) the *trans* ring of the resting state complex [*cis*GroEL7-(ADP-BeF3)7-GroES7]–[*trans*GroEL7-(ADP-BeF3)7] in syringe A was mixed with 0.5 mM ATP, 2.25 μM GroESF5M, and MDHQSY7 of varying concentrations (syringe B). The traces of different [MDHQSY7] applied are identified as red, 0.13 μM; green, 0.19 μM; purple, 0.25 μM; navy blue, 0.51 μM; and orange, 0.64 μM for *A* and *C*; for *B*, red, 0.13 μM; green, 0.25 μM; purple, 0.38 μM; navy blue, 0.51 μM; and orange, 0.64 μM; and for *D*, red, 0.028 μM; green, 0.057 μM; purple, 0.114 μM; navy blue, 0.228 μM; and orange, 0.428μM. In *A*–*D* the royal blue trace was obtained by preincubating SP-accepting species with 0.286 μM MDHQSY7and BeF3 before introducing GroESF5M and ATP. This trace of each panel was set as the 100% encapsulation level to which the equilibrium level of the all of the other traces in the same panel were normalized and converted to the fraction of GroEL ring occupied by SP as plotted in Fig. 3*B*. AU, arbitrary units.

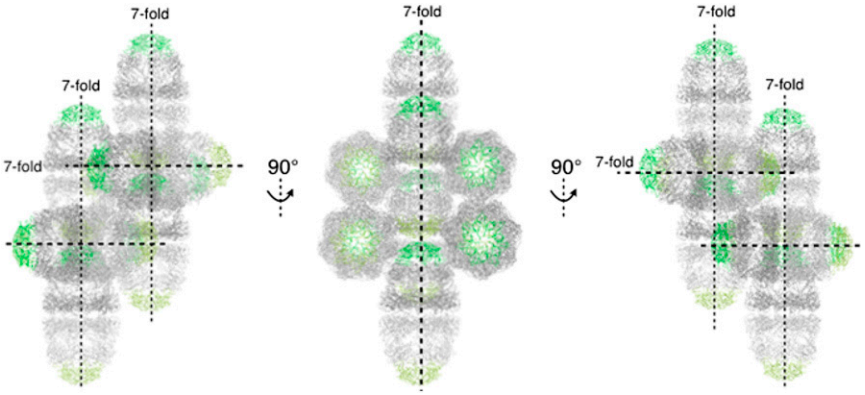

Fig. S4. Packing of the football complex in the crystal. Both the MT football and SP football are packed in the same way in the crystals. GroEL is shown in gray and GroES in green/lime.

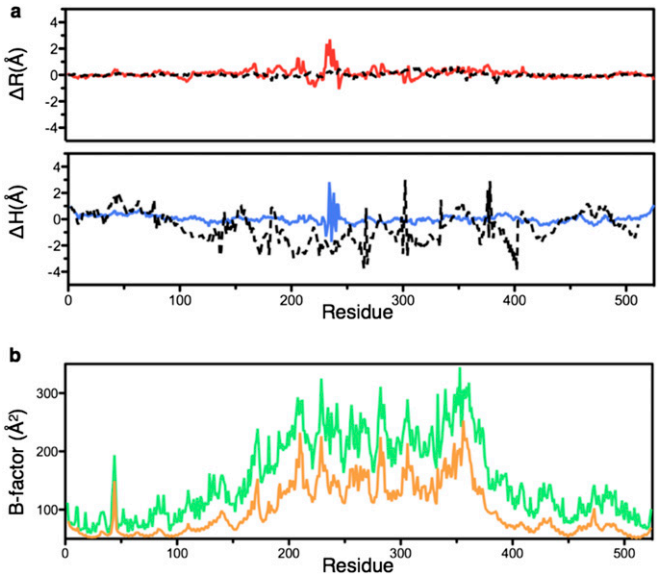

Fig. S5. Quantitative analysis of the conformational differences between MT football and SP football. (*A*) We use a cylindrical coordinate system to analyze the changes of inter-ring interface (1). $\Delta R = \langle R \rangle - \langle R' \rangle$, where R is the distance from Cα to the sevenfold axle in the MT-football complex and R′ is the corresponding distance in the SP-football complex. < > denotes average over 14 subunits. Similarly, $\Delta H = \langle H \rangle - \langle H' \rangle$, where H is the distance from Cα to the twofold axle between rings in the MT-football complex and H′ is the corresponding distance in the SP-football complex. < > denotes average over 14 subunits. ΔR and ΔH between two T-state structures (PDB ID codes 1xck and 2nwc) serves as negative control, showing the level of structural "noise." (*B*) Averaged B factors of the Cα of each residue in the MT-football (green) and SP-football (orange) complexes.

1. Fei X, Yang D, LaRonde-LeBlanc N, Lorimer GH (2013) Crystal structure of a GroEL-ADP complex in the relaxed allosteric state at 2.7 Å resolution. *Proc Natl Acad Sci USA* 110(32):E2958–E2966.

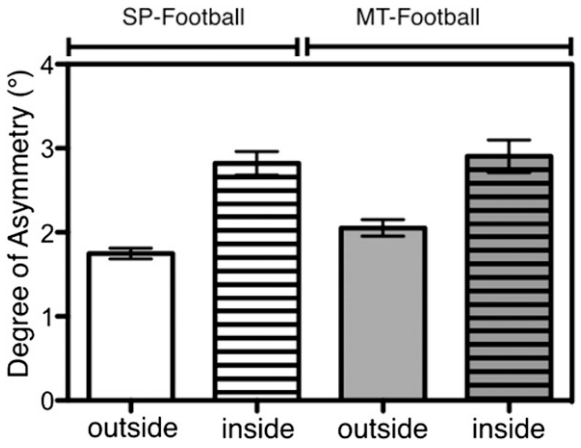

Fig. S6. Solvent-exposed residues inside the central chamber are more asymmetric than those outside the chamber. Histograms showing the average deviations from perfect sevenfold symmetry ($\theta = 360°/7 = 51.4°$) for residues exposed to the inside and outside the central chambers of SP football and MT football. The error bars show SEM.

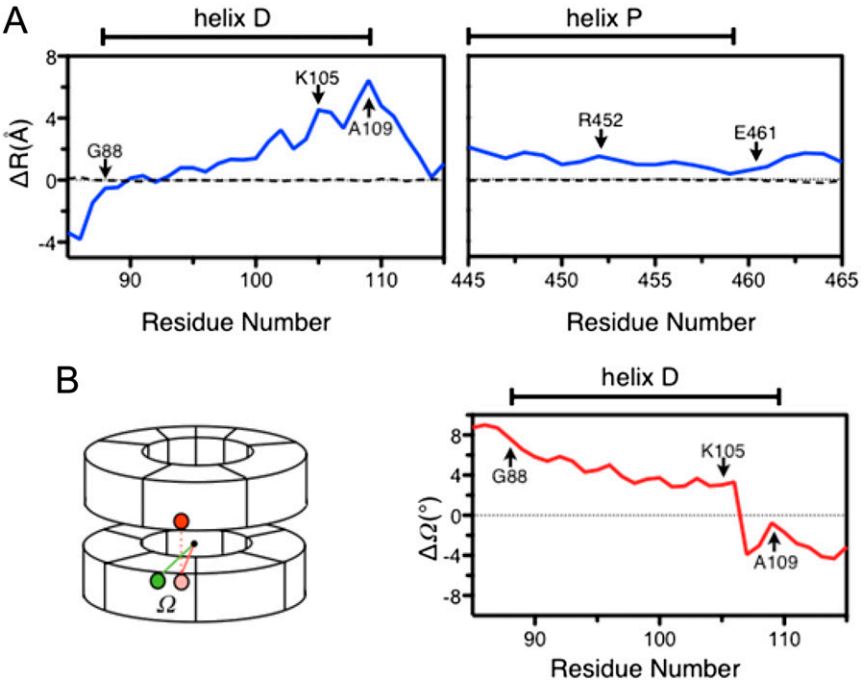

Fig. S7. Quantitative analysis of the conformational changes at the inter-ring interface during the football-to-bullet transition. (*A*) We use a cylindrical coordinate system to analyze the changes of inter-ring interface (1). $\Delta R = <R> - <R'>$, where R is the distance to the sevenfold axle in the football complex and R′ is the corresponding distance in the bullet complex. < > denotes average over seven subunits. (*B*) Definition of Ω, the quantity used to measure ring-to-ring rotation. Ω is the angle between two vectors, one from the Ca of residue *i* in subunit *j*, to the sevenfold axles of symmetry, and another from the Ca of residue *i* to the sevenfold axles of symmetry, in the subunit form L interface with subunit *j*, from the opposite ring. $\Delta\Omega = <\Omega> - <\Omega'>$, where Ω is the ring-to-ring angle in the football complex and Ω′ is the corresponding angle in the bullet complex. < > denotes average over seven L interfaces.

1. Fei X, Yang D, LaRonde-LeBlanc N, Lorimer GH (2013) Crystal structure of a GroEL-ADP complex in the relaxed allosteric state at 2.7 Å resolution. *Proc Natl Acad Sci USA* 110(32):E2958–E2966.

Table S1. Data collection and refinement statistics

Statistics	MT football	SP football
Data collection		
Space group	P 21 21 21	P 21 21 21
Cell dimensions		
a, *b*, *c*, Å	169.79, 174.49, 410.16	171.75, 173.65, 411.27
α, β, γ, °	90, 90, 90	90, 90, 90
Resolution, Å	90.9–3.84 (3.91–3.84)	122.19–3.66 (3.86–3.66)
R_{merge}, %	2.9 (70)	18.6 (65.5)
$I/\sigma I$	9.2 (2.8)	6.9 (2.34)
Completeness, %	100 (100)	98.9 (99.2)
Redundancy	7.2 (7.3)	6.1 (6.4)
Refinement		
Resolution, Å	3.84	3.66
No. of reflections	842,530	826,508
R_{work}/R_{free}	0.183/0.248	0.188/0.241
No. of atoms		
Protein	64,093	64,117
Ligand/ion	462	462
Water	0	0
B factors		
Protein	161.1	106.9
Ligand/ion	91.1	51.9
Rmsd		
Bond lengths, Å	0.008	0.006
Bond angles, °	1.1	1.2

A single native crystal was used to determine each structure. Values in parentheses are for the highest-resolution shell.